# Phase-Front Solutions and Instabilities in Forced Oscillations

Christian Elphick,[1] Aric Hagberg,[2] and Ehud Meron[3]

[1]*Centro de Fisica No Lineal y Sistemas Complejos de Santiago, Casilla 17122, Santiago, Chile*

[2]*Theoretical Division and Center for Nonlinear Studies, MSB284, Los Alamos National Laboratory, Los Alamos, NM 87545*

[3]*The Blaustein Institute for Desert Research and the Physics Department, Ben-Gurion University, Sede Boker Campus 84990, Israel*

Abstract

We study extended oscillatory systems that respond to uniform periodic forcing at one quarter of the forcing frequency. We find a new type of front instability where a stationary front shifting the oscillation phase by $\pi$ decomposes into a pair of traveling fronts each shifting the phase by $\pi/2$. The instability designates a transition from standing two-phase patterns, involving alternating domains with a phase shift of $\pi$, to traveling four-phase patterns. A generalization of the instability to higher resonances is conjectured.

29 July 1999

## I INTRODUCTION

Recent experiments on the oscillating Belousov-Zhabotinsky (BZ) reaction, subjected to time-periodic illumination, show a variety of multi-phase patterns [1]. When the forcing (illumination) frequency is roughly twice the reaction's natural frequency (2:1 resonance) two-phase patterns appear. They consist of alternating domains with oscillation phases shifted by $\pi$. Three-phase patterns appear in the 3:1 resonance and four-phase patterns in the 4:1 resonance [2]. The theory of forced oscillations within the 2:1 resonance and close to the Hopf bifurcation is well established [3, 4, 5, 6]. Front solutions that shift the phase by $\pi$, hereafter "$\pi$-fronts" , undergo a pitchfork bifurcation as the forcing strength is decreased: a stationary $\pi$-front loses stability to a pair of stable counter-propagating front solutions. The bifurcation, known as the nonequilibrium Ising-Bloch (NIB) bifurcation, designates a transition from standing two-phase patterns to traveling two-phase patterns [7, 8, 9, 10] . The NIB bifurcation appears in bistable non-oscillatory systems as well. Examples include liquid crystals subjected to rotating magnetic fields [11, 12, 13, 14], the ferrocyanide-iodate-sulfite reaction [15, 16], and catalytic surface reactions [17].

Stationary $\pi$-fronts exist in higher even resonances, 4:1, 4:3, 6:1 etc., and are stable for large enough forcing strengths. These higher resonances possess multiple stable phase states, four in the 4:1 and 4:3 resonances, six in the 6:1 resonance, and so on. Yet, in the parameter range where the $\pi$-fronts are stable, two-phase patterns prevail. Patterns involving all stable phases, like the four-phase spiral in Fig. 4a, appear only when $\pi$-fronts become unstable. We have studied this instability and found it is a degenerate instability where a stationary $\pi$-front in a $2n$:1 resonance ($n > 1$) *decomposes* into $n$ traveling $\pi/n$ fronts, each shifting the oscillation phase by $\pi/n$. The instability designates a transition from standing two-phase patterns to traveling $n$-phase patterns.

We analyze the decomposition instability in detail for the 4:1 resonance. Consider an extended system that is close to a Hopf bifurcation and externally forced with a frequency about four times larger than the Hopf frequency. The set of dynamical fields $\mathbf{u}$ describing the spatio-temporal state of the system (e.g. set of concentrations in the BZ reaction) can be written as $\mathbf{u} = \mathbf{u_0} A \exp(i\frac{\omega_f}{4}t) + c.c. + \ldots$, where $\mathbf{u_0}$ is constant, $A$ is a slowly varying complex amplitude, $\omega_f$ is the forcing frequency and the ellipses denote smaller contributions. The equation for the amplitude $A$ can be written in the following standard form (after rescaling and shifting $\arg(A)$ by a constant phase) [18, 19, 20, 21]:

$$A_\tau = (\mu + i\nu)A + (1 + i\alpha)A_{zz} - (1 - i\beta)|A|^2 A + \gamma_4 A^{*3}\,, \tag{1}$$

where the subscripts $\tau$ and $z$ denote partial derivatives with respect to time and space, and all the parameters are real. The proximity to the Hopf bifurcation implies $\mu << 1$. We will also be using the following form of Eq. (1) obtained by rescaling time, space, and amplitude as $t = \mu\tau$, $x = \sqrt{\mu/2}z$, and $B = A/\sqrt{\mu}$:

$$B_t = (1 + i\nu_0)B + \frac{1}{2}(1 + i\alpha)B_{xx} - (1 - i\beta)|B|^2 B + \gamma_4 B^{*3}\,, \tag{2}$$

where $\nu_0 = \nu/\mu$.

## II Π AND Π/2-FRONT SOLUTIONS

Consider first the gradient version of Eq. (2) obtained by setting $\nu_0 = \alpha = \beta = 0$:

$$B_t = B + \frac{1}{2}B_{xx} - |B|^2 B + \gamma_4 B^{*3}\,. \tag{3}$$

Equation (3) has four stable phase states for $0 < \gamma_4 < 1$ shown by solid circles in Fig. 1: $B_{\pm 1} = \pm\lambda$ and $B_{\pm i} = \pm i\lambda$, where $\lambda = 1/\sqrt{1 - \gamma_4}$ [22]. Front solutions connecting pairs of these states divide into two groups, $\pi$-fronts and $\pi/2$-fronts. The $\pi$-fronts, shown in Fig. 1 as solid lines, are given by

$$B_{-1\to+1} = B_{+1}\tanh x\,, \qquad B_{-i\to+i} = B_{+i}\tanh x\,. \tag{4}$$

The $\pi/2$-fronts are shown in Fig. 1 by the dashed curves. For the particular parameter value $\gamma_4 = 1/3$ they have the simple forms

$$\begin{aligned} B_{+1\to+i} &= \frac{1}{2}\sqrt{\frac{3}{2}}\,[1 + i - (1 - i)\tanh x]\,, \qquad B_{-1\to-i} = -B_{+1\to+i}\,, \\ B_{-i\to+1} &= \frac{1}{2}\sqrt{\frac{3}{2}}\,[1 - i + (1 + i)\tanh x]\,, \qquad B_{+i\to-1} = -B_{-i\to+1}\,, \end{aligned}$$

Additional front solutions follow from the invariance of Eq. (3) under reflection, $x \to -x$. For example, the symmetric counterparts of $B_{+i\to+1}(x)$ and $B_{+1\to-i}(x)$ are $B_{+1\to+i}(x) = B_{+i\to+1}(-x)$ and $B_{-i\to+1}(x) = B_{+1\to-i}(-x)$.

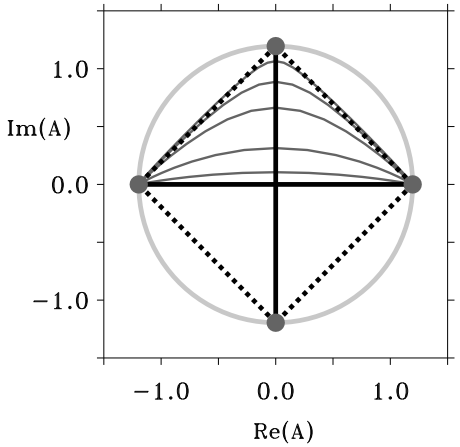


FIG. 1: Uniform states and front solutions of Eq. (3) in the complex $B$ plane. The dots represent the four spatially uniform phase states. The solid lines are the $\pi$ front solutions and the dashed lines are the $\pi/2$ fronts. The thin lines in the circle are phase portraits of front solutions at successive time steps showing the collapse of a $\pi$ front into a pair of $\pi/2$ fronts.

Consider now the nongradient system (2). The main effect of small nongradient terms is to make the $\pi/2$-fronts traveling. The nongradient terms have no effect on the $\pi$-fronts which remain stationary. To see this assume a traveling solution $B(x-ct)$ of Eq. (2) and project this equation on the translational mode $B'$. For $\pi$-fronts the resulting condition gives $c=0$. For $\pi/2$-fronts with $\gamma_4 = 1/3$ we find $|c| = \frac{3}{2}(\nu_0 - \beta)$. A perturbation analysis around $\gamma_4 = 1/3$ shows that this expression for the speed remains valid for small deviations of $\gamma_4$ from $1/3$.

## III THE DECOMPOSITION INSTABILITY

The $\pi$-fronts (4) are similar to the stationary $\pi$-front in the 2:1 resonance and like the latter become unstable as the forcing strength $\gamma_4$ is decreased. Stability analysis of the $\pi$-fronts indicates that the instability occurs at $\gamma_4 = 1/3$. The nature of the instability, however, is quite different from the NIB pitchfork bifurcation. It is a degenerate instability leading to asymptotic solutions that are not smooth continuations of the unstable stationary $\pi$-fronts. Figure 2(left) shows a space-time plot of $\arg(A)$ obtained by numerical solution of Eq. (1). The initial unstable $\pi$-front decomposes into a pair of $\pi/2$-fronts traveling to the right or to the left depending on initial conditions. Along with the $\pi$-front decomposition an intermediate phase state (the grey domain) appears. This behavior is found *arbitrarily close* to the instability point, and in this sense the new solutions are not smooth continuations of the $\pi$-front solution. To demonstrate the decomposition instability in a reaction-diffusion system we show in Fig. 2(right) a simulation of a forced FitzHugh-Nagumo model ([23]) exhibiting the same behavior as the amplitude equation (1).

We analyze first the gradient version (3). Introducing the new variables $U = Re(B) + Im(B)$ and

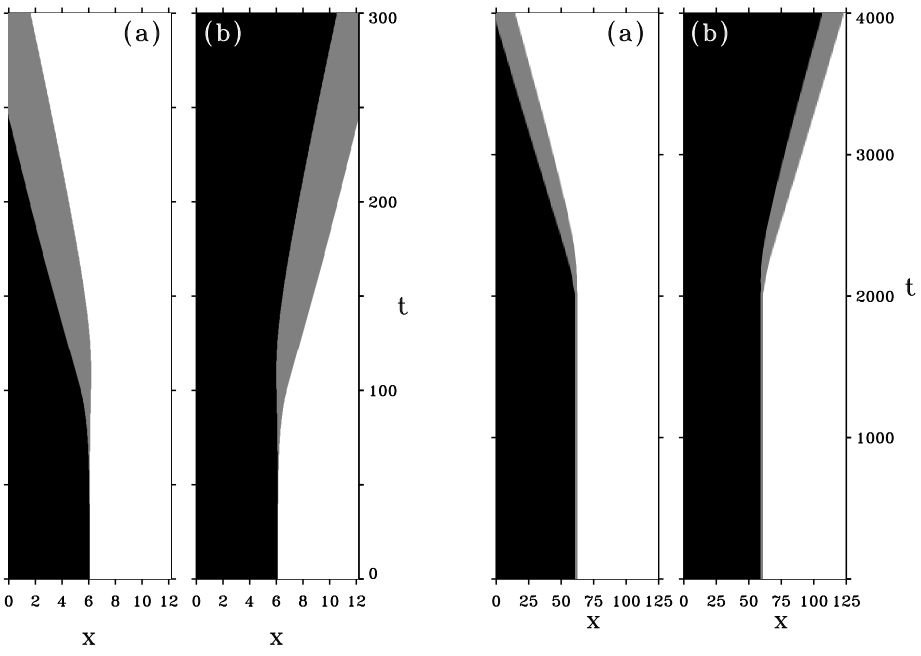


FIG. 2: Space-time plots demonstrating the decomposition instability in the 4:1 resonance. An unstable $\pi$-front decomposes into a pair of $\pi/2$-fronts traveling to the left (a) or to the right (b). The $\pi/2$-fronts enclose grey colored domains whose oscillation phases are shifted by $\pi/2$ with respect to the black and white domains. Left: Solutions of Eq. (1) showing $\arg(A)$. Parameters: $\mu = 1.0$, $\nu = 0.02$, $\gamma_4 = 0.3$, $\alpha = \beta = 0$. Right: Solutions of the forced FitzHugh-Nagumo equation showing $\arg(v/u)$. Parameters:$\epsilon = 1.9$, $b_3 = 1.8$ $\omega_f = 4.0$.

$V = Re(B) - Im(B)$ Eq. (3) is written as

$$U_t = U + \frac{1}{2}U_{xx} - \frac{2}{3}U^3 - \frac{d}{2}(U^2 - 3V^2)U\,, \tag{5a}$$

$$V_t = V + \frac{1}{2}V_{xx} - \frac{2}{3}V^3 - \frac{d}{2}(V^2 - 3U^2)V\,, \tag{5b}$$

where $d = \gamma_4 - 1/3$. At the instability point, $\gamma_4 = 1/3$, the two equations decouple (since $d = 0$) and admit solutions of the form $U = \sigma_1 B_0(x - x_1)$, $V = \sigma_2 B_0(x - x_2)$, where $B_0(x) = \sqrt{\frac{3}{2}}\tanh x$, $\sigma_{1,2} = \pm 1$, and $x_1$ and $x_2$ are arbitrary constants. An intuitive understanding of this family of solutions can be obtained by expressing these solutions back in terms of the complex amplitude $B$. For $\sigma_1 = -\sigma_2 = 1$ for example, we find

$$B(x; x_1, x_2) = B_{-i\to+1}(x - x_1) + B_{+1\to+i}(x - x_2) - \lambda\,.$$

When $|x_2 - x_1| \to \infty$ this form approaches a pair of isolated $\pi/2$-fronts:

$$B \approx B_{-i\to+1}(x - x_1) \qquad x \approx x_1\,, \qquad \text{and} \qquad B \approx B_{+1\to+i}(x - x_2) \qquad x \approx x_2\,.$$

When $x_2 - x_1 = 0$ it reduces to the $\pi$-front $B_{-i\to+i}$. Defining a mean position, $\zeta$, and an order parameter, $\chi$, by

$$\zeta = \frac{1}{2}(x_1 + x_2)\,, \qquad \chi = \frac{1}{2}(x_2 - x_1)\,,$$

the one-parameter family of solutions, $\{\tilde{B}(x;\zeta,\chi) \mid \chi \in R\}$, where $\tilde{B}(x;\zeta,\chi) = B(x;x_1,x_2)$, represents $\pi/2$-front pairs with distances, $2\chi$, ranging from zero to infinity.

For $|\gamma_4 - 1/3| = |d| \ll 1$, the weak coupling between the two equations (5a) and (5b) induces slow drift along the solution family $B(x;x_1,x_2)$. A pair solution is now written as

$$U = \sigma_1 B_0[x - x_1(t)] + u\,, \qquad V = \sigma_2 B_0[x - x_2(t)] + v\,, \tag{6}$$

where $u$ and $v$ are corrections of order $d$. Equations of motion for $x_1$ and $x_2$ or for $\zeta$ and $\chi$ follow by inserting these forms in Eqs. (5) and applying solvability conditions at order $d$:

$$\dot{\zeta} = 0, \qquad \dot{\chi} = -dV/d\chi\,. \tag{7}$$

Typical forms of the potential $V$ for positive and negative values of $d = \gamma_4 - 1/3$ are shown in Fig. 3. For $d = 0$ $V$ is identically zero. There is only one extremum point, $\chi = 0$, of $V$ for $d \neq 0$. For $d > 0$ it is a minimum and $\chi$ converges to zero. Pairs of $\pi/2$-fronts with arbitrary initial separation, $x_2 - x_1$, attract one another and eventually collapse to a single $\pi$-front ($x_1 = x_2$ or $\chi = 0$). In practice, the collapse process is noticeable only for relatively small separations. For $d < 0$ the extremum point, $\chi = 0$, is a maximum and $\chi$ diverges to $\pm\infty$. A $\pi$-front decomposes into a pair of $\pi/2$-fronts which repel one another as shown in Fig. 2 for the nongradient system (1). In the gradient case both $\pi$ and $\pi/2$-fronts are stationary (in the absence of interactions). Since the potential $V(\chi)$ becomes practically flat at finite $\chi$ values, the pair of $\pi/2$-fronts do not further depart from one another at long times.

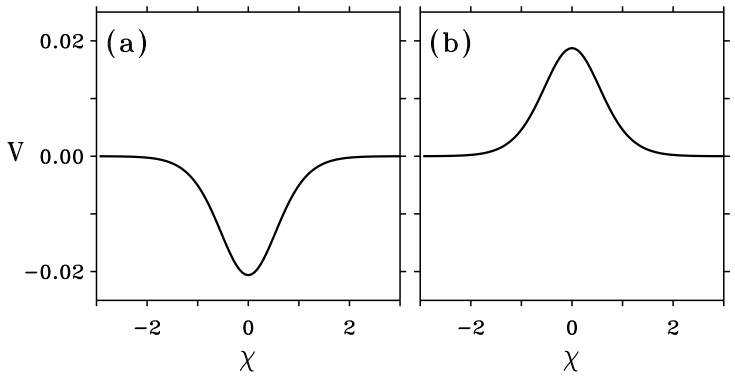


FIG. 3: The potential $V(\chi)$. (a) For $d > 0$ the extremum at $\chi = 0$ is a minimum and $\chi$ converges to 0 (a $\pi$-front). (b) For $d < 0$ the extremum is a maximum and $\chi$ diverges to $\pm\infty$ (isolated pair of $\pi/2$-fronts).

Figure 1 shows the decomposition process of a $\pi$-front in the complex $B$ plane. Starting with the $B_{-1\to+1}$ $\pi$-front, represented by the thick solid phase portrait, the time evolution (thin solid phase portraits) is toward the fixed point $B_{+i}$ and the dashed phase portraits representing the pair of $\pi/2$-fronts

$B_{+1\to+i}$ and $B_{+i\to-1}$. Because of the parity symmetry $\chi \to -\chi$, an appropriate perturbation of the initial $B_{-1\to+1}$ $\pi$-front could have led the dynamics toward the pair $B_{+1\to-i}$ and $B_{-i\to-1}$. Notice that for $d = 0$, $\dot{\zeta} = 0$, $\dot{\chi} = 0$, and we recover the two-parameter family of pair solutions $B(x;\zeta,\chi)$ with arbitrary $\zeta$ and $\chi$.

The derivation of Eqs. (7) can easily be extended to the nongradient case assuming $\nu_0$, $\alpha$ and $\beta$ are small. The $\chi$ equation remains unchanged. The $\zeta$ equation takes the form

$$\frac{\sigma_2}{\sigma_1}\dot{\zeta} = \nu F_\nu(\chi) + \alpha F_\alpha(\chi) + \beta F_\beta(\chi)\,, \tag{8}$$

where $F_\nu$, $F_\alpha$, and $F_\beta$ are odd functions of $\chi$ and do not vanish when $d = 0$ [24]. When $|\chi| \to \infty$ the right hand side of Eq. (8) converges to $\frac{3}{2}(\nu_0 - \beta)$, the speed of a $\pi/2$-front solution of Eq. (2). The $\chi = 0$ solution (representing a $\pi$-front) remains stationary ($\dot{\zeta} = 0$) in the nongradient case as well. At $\gamma_4 = 1/3$ ($d = 0$) it loses stability and decomposes into a pair of $\pi/2$-fronts which approach the asymptotic speed $\frac{3}{2}(\nu_0 - \beta)$.

The degeneracy of solutions at $\gamma_4 = 1/3$ is lifted by adding higher order terms to the amplitude equation (2). These terms are smaller by a factor of $\mu \ll 1$ than the terms appearing in (2) and their effect is noticeable only in a $\mu$-neighborhood of $\gamma_4 = 1/3$. Apart from this small parameter range the overall behavior does not change [24].

Numerical studies of amplitude equations for higher resonances suggest the existence of $\pi$-front decomposition instabilities in $2n : 1$ resonances with $n > 1$. We refer the reader to Ref. [24, 25] for demonstrations of decompositions instabilities within the 6:1 and 8:1 resonances.

## IV THE DECOMPOSITION INSTABILITY AND PATTERN DYNAMICS

The implications of the decomposition instability on pattern dynamics follow from the potentials drawn in Fig. 3 and from Eq. (8). For $\gamma_4 > 1/3$ ($d > 0$) the potential has a single minimum. $\pi/2$-fronts attract one another and collapse into stationary $\pi$-fronts. As a result standing two-phase patterns are stable. When $\gamma_4$ is decreased below 1/3 ($d < 0$) the potential acquires a single maximum and $\pi/2$-fronts repel one another. Since $\pi/2$-fronts travel, standing two-phase patterns destabilize into four-phase traveling waves. Figure 4 shows the destabilization of a four-phase spiral wave back into a standing two-phase pattern as $\gamma_4$ is increased past 1/3. The destabilization begins at the spiral core where $\pi/2$-front interactions are strongest.


## ACKNOWLEDGMENTS

We thank J. Guckenheimer, B. Krauskopf, H.L. Swinney, A. Lin, and M. Bertram for helpful discussions. This study was supported in part by grant No. 95-00112 from the US-Israel Binational Science Foundation (BSF) and by the Department of Energy, under contract W-7405-ENG-36.

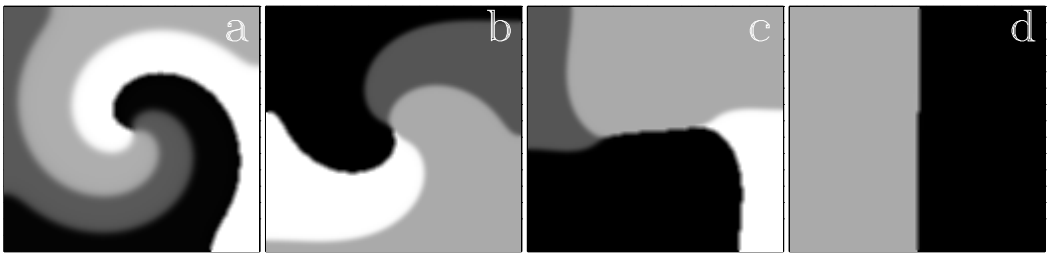


FIG. 4: Numerical solution of a two-dimensional version of Eq. (1) showing the collapse of a rotating four-phase spiral-wave into a stationary two-phase pattern. The frames show $\arg(A)$ in the $x-y$ plane. (a) The initial four-phase spiral wave (computed with $\gamma_4 < 1/3$). (b) The spiral core, a 4-point vertex, splits into two 3-point vertices connected by a $\pi$-front. (c) A two-phase pattern develops as the 3-point vertices further separate. (d) The final stationary two-phase pattern. Parameters: $\gamma_4 = 0.6$, $\mu = 1$, $\nu_0 = 0.1$, $\alpha = \beta = 0$, $x = [0, 64]$, $y = [0, 64]$.

## REFERENCES


[1] V. Petrov, Q. Ouyang, and H. L. Swinney, Nature **388**, 655 (August 1997).

[2] A. Lin and H. L. Swinney, *Center for Nonlinear Dynamics*, *UT Austin*, personal communication.

[3] P. Coullet, J. Lega, B. Houchmanzadeh, and J. Lajzerowicz, Phys. Rev. Lett. **65**, 1352 (1990).

[4] P. Coullet and K. Emilsson, Physica D **61**, 119 (1992).

[5] B. A. Malomed and A. A. Nepomnyashcy, Europhys. Lett. **27**, 649 (1994).

[6] D. Walgraef, *Spatio-Temporal Pattern Formation* (Springer-Verlag, New York, 1997).

[7] A. Hagberg and E. Meron, Nonlinearity **7**, 805 (1994), http://math.lanl.gov/People/aric/Papers/frontbif/.

[8] H. Ikeda, M. Mimura, and Y. Nishiura, Nonl. Anal. TMA **13**, 507 (1989).

[9] M. Bode, A. Reuter, R. Schmeling, and H.-G. Purwins, Phys. Lett. A **185**, 70 (1994).

[10] C. Elphick, A. Hagberg, E. Meron, and B. Malomed, Phys. Lett. A **230**, 33 (1997), http://math.lanl.gov/People/aric/Papers/forced/.

[11] K. B. Migler and R. B. Meyer, Physica D **71**, 412 (1994).

[12] T. Frisch, S. Rica, P. Coullet, and J. M. Gilli, Phys. Rev. Lett. **72**(10), 1471 (1994).

[13] S. Nasuno, N. Yoshimo, and S. Kai, Phys. Rev. E **51**, 1598 (1995).

[14] T. Frisch and J. M. Gilli, J. Phys. II France **5**, 561 (1995).

[15] K. J. Lee and H. L. Swinney, Phys. Rev. E **51**(3), 1899 (1995).

[16] D. Haim, G. Li, Q. Ouyang, W. D. McCormick, H. L. Swinney, A. Hagberg, and E. Meron, Phys. Rev. Lett. **77**(1), 190 (July 1996), http://math.lanl.gov/People/aric/Papers/breathing/.

[17] G. Haas, M. Bär, I. G. Kevrekidis, P. B. Rasmussen, H.-H. Rotermund, and G.Ertl, Phys Rev. Lett. **75**, 3560 (1995).

[18] A. C. Newell, in *Lectures in Applied Mathematics* (American Mathematical Society, Providence, RI, 1974), vol. 15, p. 157.

[19] J. M. Gambaudo, J. Diff. Eq. **57**, 172 (1985).

[20] C. Elphick, G. Iooss, and E. Tirapegui, Phys. Lett. A **120**, 459 (1987).

[21] M. C. Cross and P. C. Hohenberg, Rev. Mod. Phys. **65**(3), 851 (1993).

[22] B. Krauskopf, *On the 1:4 Resonance Problem*, Ph.D. thesis, Rijksuniversiteit Groningen (June 1995).

[23] The model is $u_t = u - (1 + b_3 sin(\omega_f t))u^3 - v + u_{xx}, v_t = \epsilon(u - v/2)$.

[24] C. Elphick, A. Hagberg, and E. Meron, Phys. Rev. E **59**(5), 5285 (1999), http://math.lanl.gov/People/aric/Papers/fcgl2/.

[25] C. Elphick, A. Hagberg, and E. Meron, Phys. Rev. Lett. **80**(22), 5007 (1998), http://math.lanl.gov/People/aric/Papers/fcgl/.